Supplementary information for

Substantial Expansion of Detectable Size Range in Ionic Current Sensing through Pores by Using a Microfluidic Bridge Circuit

Hirotoshi Yasaki[1,2], Takao Yasui[1,2,3*], Takeshi Yanagida[4,5*], Noritada Kaji[1,2], Masaki Kanai[4], Kazuki Nagashima[4], Tomoji Kawai[5*], and Yoshinobu Baba[1,2,6*]*

[1]Department of Biomolecular Engineering, Graduate School of Engineering, Nagoya University, Furo-cho, Chikusa-ku, Nagoya 464-8603, Japan

[2]ImPACT Research Center for Advanced Nanobiodevices, Nagoya University, Furo-cho, Chikusa-ku, Nagoya 464-8603, Japan

[3]Japan Science and Technology Agency (JST), PRESTO, 4-1-8 Honcho, Kawaguchi, Saitama 332-0012, Japan

[4]Laboratory of Integrated Nanostructure Materials Institute of Materials Chemistry and Engineering, Kyushu University, 6-1 Kasuga-koen, Kasuga, Fukuoka 816-8580, Japan

[5]Institute of Scientific and Industrial Research, Osaka University, Mihogaoka, Ibaraki 567-0047, Osaka, Japan

[6]Health Research Institute, National Institute of Advanced Industrial Science and Technology (AIST), Takamatsu 761-0395, Japan

This file includes:

1. Supplementary Figures (Figs. S1-S3)
2. Derivation and validation of theoretical equation (Fig. S4)
3. Validation of accuracy of 200 nm particle detection result

1. Supplementary Figures

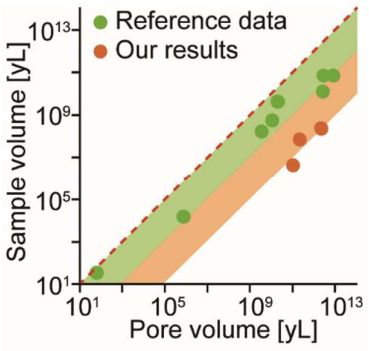

Figure S1. Detectable particle volumes reported in the literature and our results. Green dots show reported data points obtained by conventional methods[2, 4, 5, 14, 22-25] and the green band shows their reported detection range. Orange dots and band showing our data points and our detection range. The red dotted line represents the 100% pore volume. The reported methods have the inherent limitation of detectable samples of a 1 % pore volume; on the other hand, our developed method achieved detection of samples of a 0.01 % pore volume.

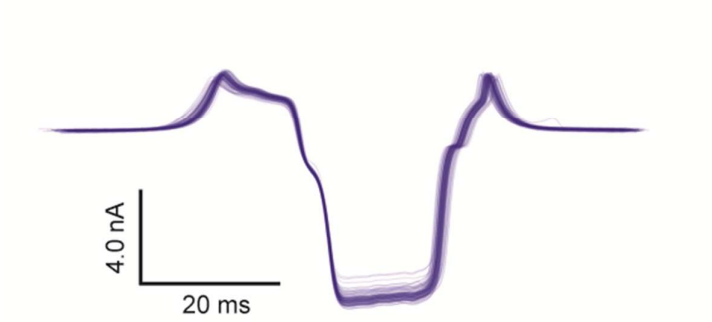

Figure S2. Overlay of 100 signals of 3.1 µm polystyrene particles. All signals had the same shape, and that proved the high reproducibility of our method. Micropore dimensions were 7.5 µm height × 4.0 µm width × 80 µm length; applied voltage, 12 V.

Translocation time in micropores.

Similar to the tendency of the conventional methods, there is a trade-off between signal amplitude and translocation time; a longer micropore shows a smaller signal amplitude and longer translocation time (Figs. S3a-3c). It should be noted, however, that our methodology would have a long enough translocation time (>200 ms) to distinguish various interactions between the sample and pores (Fig. S3d). Since translocation time of samples had a relationship to the applied electric fields or sample surface charge (Fig. S3e), our methodology would be capable of identifying biological samples based on surface charges, depending on the sample types.

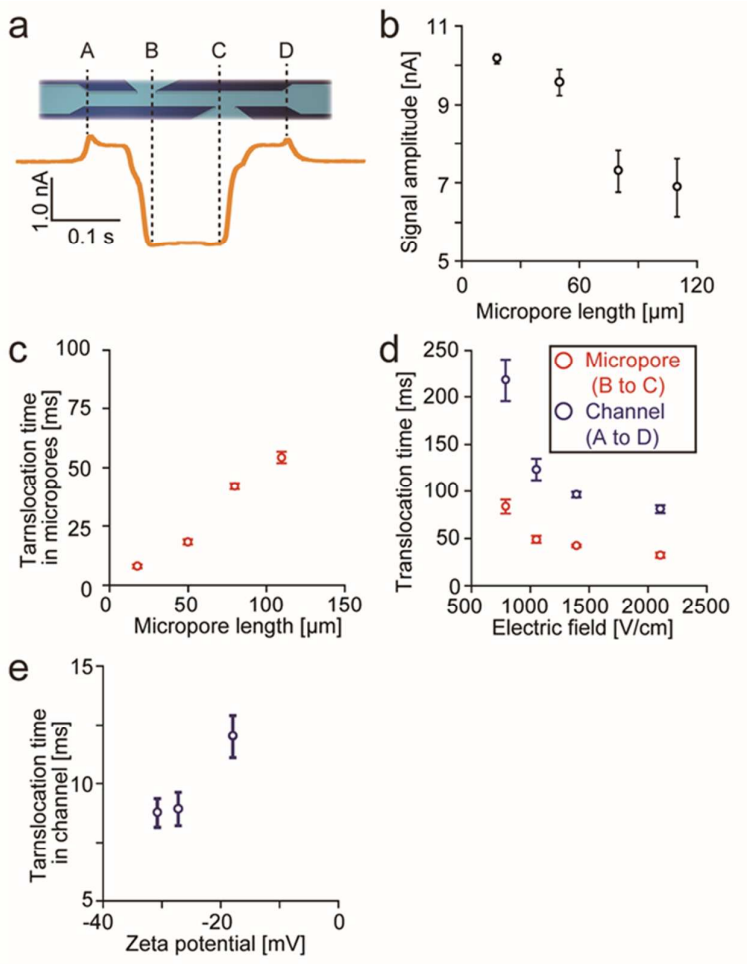

Figure S3. Translocation time in micropores. (a) A schematic illustration of the micropore and a signal for 2.08 μm diameter particles; micropore dimensions of 7.5 μm height × 4.0 μm width × 80 μm length; applied voltage, 12 V. We defined the micropore as being from positions B to C and positions A and D as showing ends of a channel including the micropore. (b, c) Signal amplitude and translocation time of 3.10 μm diameter particles; micropore dimensions of 7.5 height × 4.0 μm width. Error bars show the standard deviation for a series of measurements (N = 200). (d) A relationship between electric field and translocation time in the micropore (B to C in Fig. S2a) and in the channel (with ends at A and D in Fig. S3a). The micropore was 80 μm long and the channel was 150 μm long. Error bars show the standard deviation for a series of measurements (N = 100). (e) A relationship between zeta potential of 3.10 μm

diameter particles and translocation time in the channel (with ends at A and D in Fig. S3a); micropore dimensions of 6.6 μm height × 4.5 μm width × 16 μm length. Channel length was 40 μm.

2. Derivation of theoretical equation

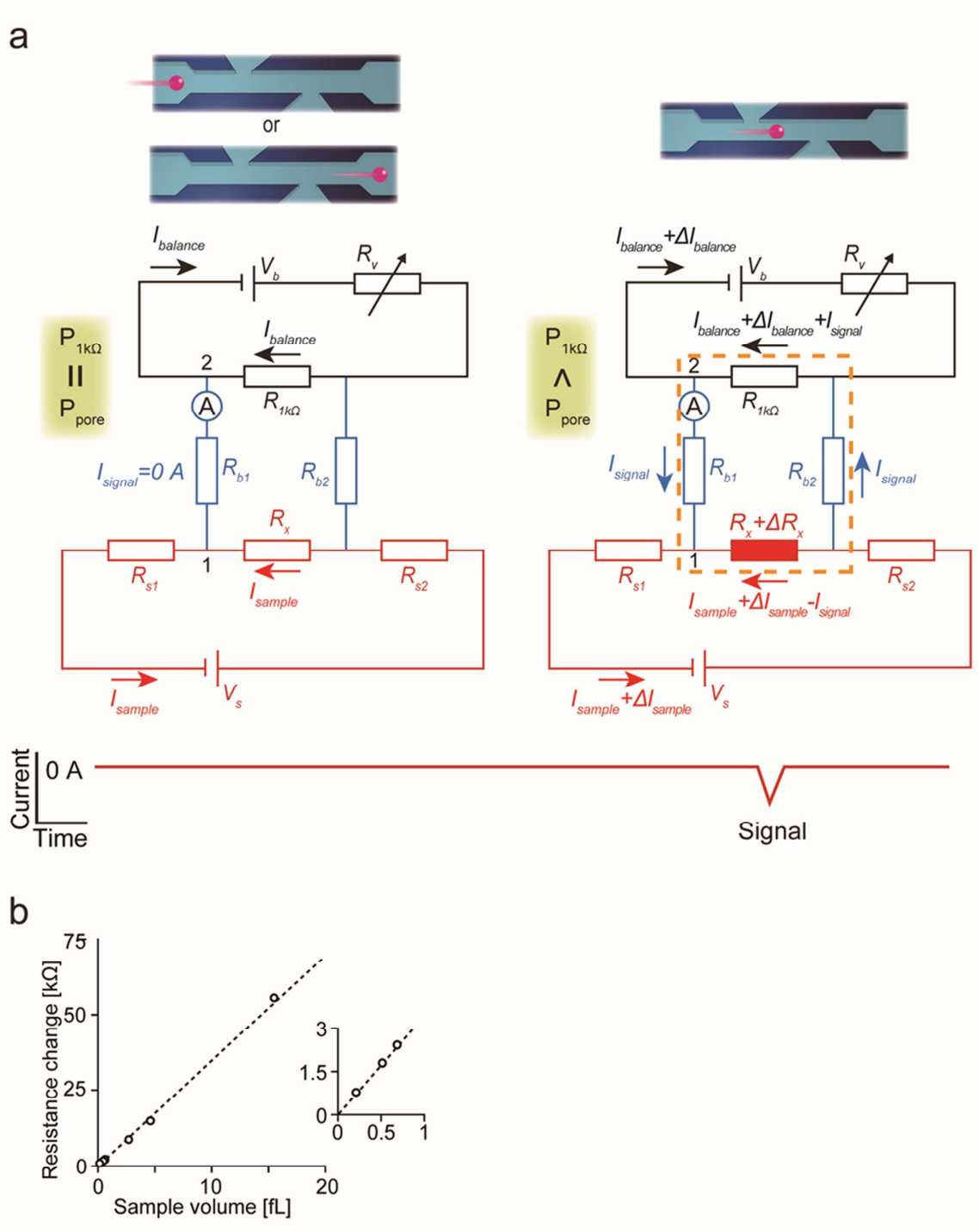

Figure S4. Schematic illustrations of the current sensing method for derivation of theoretical equation.

(a) Schematic illustrations of sample particle translocation, electric circuit diagrams, and schematic current value in the microfluidic bridge circuit. The left side shows the situation before and after passage of sample particles in the micropore. The right side shows the situation for the time of passage of the sample particles in the micropore. Red lines are for the sample circuit, blue lines are for the bridge lines, and black lines are for the balance circuit. The sample circuit has a voltage source (V_s) and resistors for the

micropore (R_x) and sample flow channels (R_{s1} and R_{s2}). The bridge lines have resistors for them (R_{b1} and R_{b2}) and an Ampere meter (A). The balance circuit has a voltage source (V_b), a variable resistor (R_v), and a 1-kΩ resistor ($R_{1\text{-}k\Omega}$). Red filled squares show increased resistance by sample introduction. Red and black arrows show flow direction of current in the sample circuit and the balance circuit, respectively. Blue arrows show flow direction of current by deviation of potential differences between the two circuits, sample and balance. The numbers "1" and "2" are the electrical potential of the micropore entrance and the electrical potential of the cathode of the voltage source in the balance circuit, respectively. $P_{1k\Omega}$ and P_{pore} are the potential differences of both ends for the 1-kΩ resistor and the micropore, respectively. (b) A relationship between particle volume and calculated resistance change of a micropore by using the equation for calculating electric resistance value of conductor; micropore dimensions of 7.5 μm height × 4.0 μm width × 80 μm length. The micropore without particles has a resistance of 6.72 MΩ. The inset figure shows an expanded image for the resistance change less than 3 kΩ. The black dotted line is the fitting curve result.

Our method uses two electrical circuits: a sample circuit and a balance circuit. We derived a theoretical equation to calculate signal amplitudes, which are detected in this method, based on Ohm's law and Kirchhoff's law. In the balanced state, no current flows in the bridge channels (situation of the left-side drawing in Fig. S3a), and the following equations are formulated for each "isolated" circuit:

$$I_{sample} = \frac{V_s}{R_{s1} + R_x + R_{s2}} \qquad (S1)$$

$$I_{balance} = \frac{V_b}{R_{1-k\Omega} + R_v} \qquad (S2)$$

where R_{s1}, R_{s2}, R_x, $R_{1\text{-}k\Omega}$, and R_v are the electrical resistances of sample flow channels, the micropore, the 1-kΩ resistor, and the variable resistor, respectively. V_f and V_p are the applied voltages for the sample and balance circuits, respectively. I_{sample} and $I_{balance}$ are currents in the sample and balance circuits, respectively. Since potential differences between both ends of the micropore (R_x) and the 1-kΩ resistor ($R_{1\text{-}k\Omega}$) are the same in the balanced state, Eqs. (S1) and (S2) are transformed as:

$$R_x \times I_{sample} = R_{1-k\Omega} \times I_{balance}. \qquad (S3)$$

When a sample is passing through the micropore, the current in the sample circuit changes from I_s to $I_{sample}+\Delta I_{sample}$:

$$I_{sample} + \Delta I_{sample} = \frac{V_s}{R_{s1} + R_x + \Delta R_x + R_{s2}} \qquad (S4)$$

where ΔR_x and ΔI_{sample} are resistance change of the micropore and current change in sample circuit by sample introduction, respectively. At the same time, the potential difference between both ends of the micropore (P_{pore}) is increased by the increasing resistance, and the signal (I_{signal}) flows to an Ampere meter to make up the potential difference between points 1and 2 (situation of the right-side drawing in Fig. S3a). At this time, the balanced state is lost. The following equation is the sum of the voltages of the circuit surrounded by the orange dotted line:

$$\left(I_{sample} + \Delta I_{sample} - I_{signal}\right)(R_x + \Delta R_x) = I_{signal}(R_{b1} + R_{b2} + R_{1-k\Omega}) + (I_{balance} + \Delta I_{balance})R_{1-k\Omega} \qquad (S5)$$

where R_{b1} and R_{b2} are the electrical resistances of the bridge channels. $\Delta I_{balance}$ is current change in sample circuit by sample introduction. The following equation is the expansion equation of eq (S5).

$$I_{sample}R_x + I_{sample}\Delta R_x + \Delta I_{sample}R_x + \Delta I_{sample}\Delta R_x - I_{balance}R_{1-k\Omega} - \Delta I_{balance}R_{1-k\Omega} = I_{signal}(R_{b1} + R_{b2} + R_{1-k\Omega} + R_x) + I_{signal}\Delta R_x \qquad (S6)$$

Since ΔI_{sample} and I_{signal} are small enough compared with I_{sample} and $I_{balance}$, the fourth term on the left side ($\Delta I_{sample}\Delta R_x$) and the second term on the right side ($I_{signal}\Delta R_x$) can be ignored, and Eq. (S6) can be transformed by Eq. (S3) as follows.

$$I_{sample}\Delta R_x \approx I_{signal}(R_{b1} + R_{b2}) + \left(I_{signal} + \Delta I_{balance}\right)R_{1-k\Omega} + \left(I_{signal} + \Delta I_{sample}\right)R_x \qquad (S7)$$

The following equation is the sum of the voltages of the black circuit.

$$V_b = R_v(I_{balance} + \Delta I_{balance}) + R_{1-k\Omega}\left(I_{balance} + \Delta I_{balance} + I_{signal}\right) \qquad (S8)$$

Equation (S8) can be transformed by Eq. (S2) as follows.

$$\Delta I_{balance} = \frac{-R_{1-k\Omega}}{R_v + R_{1-k\Omega}} \cdot I_{signal} \qquad (S9)$$

Based on Eq. (S9), the following approximate expression is obtained when R_v is large enough compared with $R_{1\text{-}k\Omega}$.

$$|\Delta I_{balance}| \ll |I_{signal}| \quad \text{(S10)}$$

The following equation is the sum of the voltages of the red circuit.

$$V_s = (I_{sample} + \Delta I_{sample})(R_{S1} + R_{S2} + R_x) - I_{signal}R_x \quad \text{(S11)}$$

When ΔR_x is small enough compared with R_x, Eq. (S11) can be transformed by Eq. (S1) as follows.

$$\Delta I_{sample} \approx \frac{R_x}{R_{S1} + R_{S2} + R_x} \cdot I_{signal} \quad \text{(S12)}$$

Based on Eq. (S12), the following approximate expression is obtained when R_x is small enough compared with $R_{s1}+R_{S2}$.

$$|\Delta I_{sample}| \ll |I_{signal}| \quad \text{(S13)}$$

Based on Eq. (S10) and Eq. (S13), Eq. (S7) can be transformed as follows.

$$I_{sample}\Delta R_x \approx I_{signal}(R_{b1} + R_{b2} + R_{1-k\Omega} + R_x) \quad (S14)$$

Therefore, the detected current signals can be theoretically predicted by Eq. (S8) (this is Eq. (1) of the main text).

$$I_{signal} = \frac{\Delta R_x}{R_{b1} + R_{b2} + R_{1-k\Omega} + R_x} \times \frac{V_s}{R_{s1} + R_{s2} + R_x} \quad (S15)$$

Channel resistances (R_{b1}, R_{b2}, R_{s1}, and R_{s2}) can be calculated by Eq. (S16):

$$R = \rho \times \frac{L}{A} \quad (S16)$$

where ρ, L, and A are the electrolyte solution resistivity, channel length, and cross-sectional area of the channels, respectively. Based on Eqs. (S15) and (S16), the signal amplitude is in proportion to the applied voltage (V_s), and in inverse proportion to the resistance of the sample circuit ($R_{S1}+R_x+R_{S2}$), the sum of the resistances of the bridge channels, the micropore, and the 1-kΩ resistor ($R_{b1}+R_{b2}+R_{1\text{-}k\Omega}+R_x$), and the electrolyte solution resistivity (ρ).

3. Validation of accuracy of 200 nm particle detection result

In the detection of 200 nm particles in the 14 μm long micropore, resistivity (ρ) of the microchannels filled with 5×TBE buffer was 0.319 kΩ•cm, resistance of the sample circuit ($R_{S1}+R_x+R_{S2}$) was 18.8 MΩ, the sum of resistances of the bridge channels, the micropore, and the 1-kΩ resistor ($R_{b1}+R_{b2}+R_{1\text{-}k\Omega}+R_x$) was 13 MΩ, applied voltage (V_s) was 53 V, and resistance change of the micropore by the 200 nm diameter particle introduction (ΔR_x) was 0.84 kΩ. Using eq (S8), we could calculate I_{signal} as 180 pA. Therefore, the detected value was accurate.